

# Resonance scattering and singularities of the scattering function

W.D. Heiss<sup>1,a</sup> and R.G. Nazmitdinov<sup>2,3</sup>

<sup>1</sup> National Institute for Theoretical Physics, Stellenbosch Institute for Advanced Study, and Institute of Theoretical Physics, University of Stellenbosch, 7602 Matieland, South Africa

<sup>2</sup> Department de Física, Universitat de les Illes Balears, 07122 Palma de Mallorca, Spain

<sup>3</sup> Bogoliubov Laboratory of Theoretical Physics, Joint Institute for Nuclear Research, 141980 Dubna, Russia

Received 20 January 2010 / Received in final form 8 March 2010

Published online 6 April 2010 – © EDP Sciences, Società Italiana di Fisica, Springer-Verlag 2010

**Abstract.** Recent studies of transport phenomena with complex potentials are explained by generic square root singularities of spectrum and eigenfunctions of non-Hermitian Hamiltonians. Using a two channel problem we demonstrate that such singularities produce a significant effect upon the pole behaviour of the scattering matrix, and more significantly upon the associated residues. This mechanism explains why by proper choice of the system parameters the resonance cross section is increased drastically in one channel and suppressed in the other channel.

## 1 Introduction

It is well established knowledge that the shape of measured cross sections, in particular that of resonances, is described satisfactorily by poles of the scattering function in the complex energy plane [1]. These poles correspond to particular solutions of the Schrödinger equation at complex energies by imposing the boundary conditions that the wave function be regular at the origin and have only outgoing waves at large distances<sup>1</sup>. They have been discussed recently again in the context of complex potentials [3]. In fact, while for a Hermitian Hamiltonian such solutions can occur only at complex energies with non-vanishing negative imaginary part<sup>2</sup>, a complex potential (associated with absorption) can give rise to such states at energies with vanishing or even positive imaginary part. As a rule, these specific solutions give rise to a pole of first order in the Green's function  $(E - H)^{-1}$  and thus in the scattering function. This remains true also in multi-channel problems, even if there is a degeneracy, where the residue of the pole is a matrix of rank larger than one.

There are, however, special singularities of the Green's function and thus of the scattering function being of a very different nature: the exceptional points (EP) of a Hamiltonian. They are also specific solutions of the Schrödinger equation or, in more general terms, of an eigenvalue problem, but for a non-Hermitian problem. They have been discussed at great length theoretically [4–8] and in a large variety of applications such as in

atomic physics [9,10], in optics [11], in nuclear physics [12] and in different theoretical context in  $\mathcal{PT}$ -symmetric models [13], to name just a few. Depending on the particular situation EPs can signal a phase transition [14,15]. The experimental verification of the existence of EPs requires a careful tuning of parameters of the particular open system investigated (see below Sect.2.2). Recently the topological structure of the square root branch point associated with an EP has been shown experimentally to be a physical reality [16–18].

While some of the quoted papers report about particular physical effects of the EPs, either expected or measured, no emphasis is placed upon the important role of the eigenstates when the vicinity of an EP is explored in the laboratory. We recall that an EP is characterised by the coalescence of not just two eigenvalues but also of their associated eigenstates; moreover, the norm of the associated eigenstate – there is only one – vanishes at the EP. It is the main purpose of the present paper to illustrate the dramatic effect of this vanishing norm upon the residues of the scattering function (which has a pole of second order at the EP [19]) resulting in a distinctly different resonance behaviour in the different channels. To facilitate the demonstration we restrict ourselves to a two-channel problem.

## 2 Sharp resonances and exceptional points

### 2.1 The model

To illuminate the basic mechanism of the sudden increase of a resonance cross section, associated with EPs, we strip the great variety of models down to the essentials and elaborate the universal cause by studying a generic model.

<sup>a</sup> e-mail: dieter@physics.sun.ac.za

<sup>1</sup> These solutions are called Gamov states; see, for example [2].

<sup>2</sup> Here we do not consider bound states occurring for negative energies for the same boundary conditions; the continuous spectrum is treated effectively using complex eigenvalues.

It is well established that, in the close vicinity of an EP, a two-dimensional matrix model suffices to capture all essential features associated with the singularity. We thus begin with the model Hamiltonian

$$H(\lambda) = H_0 + H_1(\lambda) = H_0 + \lambda V = \begin{pmatrix} \omega_1 & 0 \\ 0 & \omega_2 \end{pmatrix} + \lambda \begin{pmatrix} \epsilon_1 & \delta \\ \delta & \epsilon_2 \end{pmatrix} \quad (1)$$

where the parameters  $\omega_k$  and  $\epsilon_k$  determine the non-interacting resonance energies  $E_k = \omega_k + \lambda\epsilon_k$ ,  $k = 1, 2$ . They are chosen complex and such that the  $E_k$  have negative imaginary parts; we focus on  $\lambda$  between 0.5 and 0.6. As we are interested in the effects of crossing and coalescence in scattering, we consider in the following the scattering matrix, viz.

$$T_{i,k} = H_1(\lambda)_{i,k} + (H_1(\lambda)(E - H(\lambda))^{-1}H_1(\lambda))_{i,k}. \quad (2)$$

Since we mimic a multi-channel problem by an effective two-channel Hamiltonian, i.e.  $\omega_i$  and  $\epsilon_i$  are complex, the scattering amplitude (2) does not satisfy the unitarity condition [1].

To describe, for  $\delta = 0$ , the simultaneous observation of the two resonances in both channels on equal footing, we have to consider the scattering matrix in a basis rotated by the angle  $\pm\pi/4$  rather than in the basis given by (1). That is, the labels  $i, k$  in the scattering matrix (2) refer to the basis  $\{c1/\sqrt{2} \pm c2/\sqrt{2}, c1/\sqrt{2} \mp c2/\sqrt{2}\}$  with  $\{c1, c2\}$  being an eigenvector of (1). This specific observational basis is essential to ensure that even for the non-interacting case ( $\delta = 0$ ) both resonances are equally and simultaneously present in either channel; the difference between the two channels shows when  $\delta$  is switched on as is discussed in the following sections. We choose the parameters  $\omega_k$  and  $\epsilon_k$  for convenient demonstration, that is  $\omega_1 = 1.55 - 0.007i$ ,  $\omega_2 = 1.1 - 0.007i$ ,  $\epsilon_1 = -0.4 - 0.0006i$ ,  $\epsilon_2 = 0.4 + 0.0005i$ . The values have no particular significance, they serve to illustrate the principle, that is the effect of a near EP upon scattering; any other set that invokes crossing and coalescence of resonances would serve the same purpose as long as the imaginary parts of the poles are near to the real axis.

## 2.2 The interacting resonances

From (2) we obtain the cross sections  $\sim(TT^\dagger)_{kk}$  as a function of the energy for various values of  $\lambda$ . This is illustrated in Figure 1, where  $(TT^\dagger)_{11}$  is plotted for  $\delta = 0$ . Without coupling, when the energies cross (a usual degeneracy), the figures for  $(TT^\dagger)_{22}$  coincide with those of  $(TT^\dagger)_{11}$ . Such crossing of resonances is often associated with a particular symmetry, this aspect is of no significance for our purpose. The crossing happens at  $\lambda_{\text{cross}} = 0.5625 - 0.00077i$ .

The difference between  $(TT^\dagger)_{11}$  and  $(TT^\dagger)_{22}$  changes dramatically when the coupling  $\delta$  is turned on. In our example we have chosen a purely absorptive coupling as then the two EPs avoid the real  $\lambda$ -axis (recall that the Hamiltonian is non-Hermitian even for  $\delta = 0$  owing to the unperturbed widths; it means EPs may occur for real  $\lambda$ ).

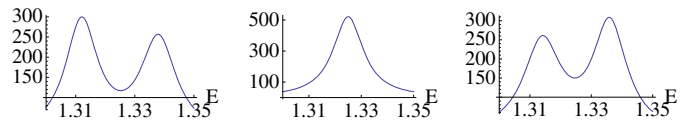


**Fig. 1.** Crossing of resonances without coupling ( $\delta = 0$ ). The three figures are taken for  $\lambda = 0.53$ ,  $\Re\lambda_{\text{cross}} = 0.5625$  and  $0.59$ , respectively. The units are arbitrary but the same for all three figures.

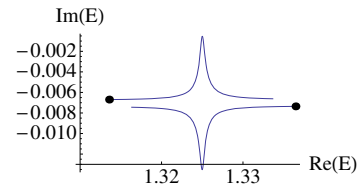


**Fig. 2.** Energy eigenvalue trajectories when  $\lambda$  sweeps from 0.53 to 0.59 for  $\delta = 0.0115i$ . If  $\delta = 0$  the straight lines continue as straight lines avoiding the peaks. Note that for our choice of parameters the trajectories run in opposite directions, the respective starting points are indicated by a dot.

For  $\delta = 0.0115i$  the EPs are at  $\lambda_+ = 0.579 - 0.00082i$  and  $\lambda_- = 0.547 - 0.00073i$  with the energies  $1.325 - 0.007029i$  and  $1.325 - 0.007027i$ , respectively. The EPs sprout from  $\lambda_{\text{cross}}$ , a critical value used below is  $\lambda_{cr} = \Re(\lambda_+ + \lambda_-)/2 \approx \lambda_{\text{cross}}$ . The dependence on any parameter is highly sensitive when  $\delta \neq 0$  owing to the proximity of the EPs invoking large derivatives of spectrum and eigenfunctions. In particular, the dependence on  $\delta$  is crucial and can change patterns as is further discussed below.

In Figure 2 we illustrate the trajectories of eigenvalues of the Hamiltonian (1) obtained by variation of  $\lambda$  for the parameter set considered above. We note the sharp deviations from the straight lines of the trajectories bringing one resonance close to the real energy axis while the other is moving into the opposite direction. The two EPs lie basically within the centre of the two peaks; at each of these points the levels behave to lowest order as  $E_{\pm} \sim E_{EP} \pm \text{const.} \sqrt{\lambda - \lambda_{EP}}$  implying a large derivative. Moreover, the state vectors have a similar strong dependence: while they are properly normalised their directions change rather swiftly when  $\lambda$  is sweeping over the critical value  $\lambda_{cr} = 0.563$ . We emphasise that the phenomenon of width repulsion associated with level crossings as illustrated in Figure 2 is usually not encountered for real values of the strength parameter  $\lambda$ . It occurs in our model as both EPs are on the same side of the real  $\lambda$ -axis being a consequence of dealing with a non-Hermitian Hamiltonian from the outset [20]. The combined effect is the dramatic change for both cross sections in the immediate vicinity of the critical point as illustrated in Figure 3.

The obvious effect is the huge increase of the cross section for  $(TT^\dagger)_{11}$  which is due to the narrow resonance. In contrast, there is a substantial drop for  $(TT^\dagger)_{22}$  in comparison with the centre figure of Figure 1. Moreover, the shape of this latter ‘‘resonance’’

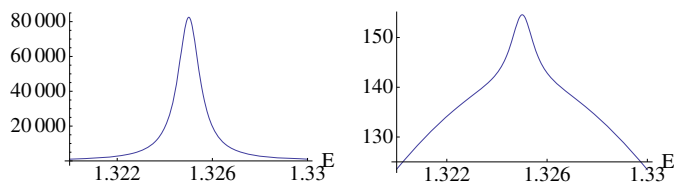


**Fig. 3.** Energy dependence of  $(TT^\dagger)_{11}$  (left) and  $(TT^\dagger)_{22}$  (right) for  $\delta = 0.0115i$  at the critical point  $\lambda_{cr} = 0.563$ . Note the huge difference in scale between the two drawings. The units are as in Figure 1.

is no longer of the usual Lorentzian type (as was first noticed in Ref. [21]). This dramatic change essentially takes place, albeit continuously, within the narrow interval  $\{\lambda_{cr} - 0.03, \lambda_{cr} + 0.03\}$ . In fact, for the same values of the coupling the curves at  $\lambda = 0.53$  or  $\lambda = 0.59$  look just like those in Figure 1, where  $\delta = 0$  is considered. This is understandable as the trajectories shown in Figure 2 are virtually unaffected by the small coupling outside the interval  $\{\lambda_{cr} - 0.03, \lambda_{cr} + 0.03\}$ . The same holds for the eigenvectors. We note that the “peak on the peak” on the right hand side of Figure 3 is again an effect of fine tuning. It is brought about by the conspiracy of the two poles and their respective residues as they occur on the top and bottom cusp in Figure 2. Decreasing for instance  $\delta$ , the “peak on the peak” can disappear but the resulting shape still is not a Lorentzian, it rather retains the flat plateau without the “second peak”.

Of course, there is nothing special about the 11-channel that becomes so strongly enhanced. When the sign of the rotational angle  $\pi/4$  is changed, the two eigenfunctions simply swap and it is then the 22-channel that appears so dramatically enhanced while the 11-channel is suppressed; similarly, as the phases of the (normalised) eigenvectors of (1) are arbitrary, changing the sign of either  $c_1$  or  $c_2$  will also swap the roles of the two channels. The important point is the strong enhancement of one channel while the other is suppressed. In either case, the effect occurs only in the immediate vicinity of  $\lambda_{cr} = 0.563$ . The pattern in Figure 3 has its origin not only in the square root branch points of the spectrum but rather in the associated eigenstates. This aspect, that is the effect of the eigenstates upon the residues of the Green’s function, is often overlooked in the literature; *it is not only the pole positions but also the strong and distinctly different variation of the two residues* that brings about the effects discussed here.

The trajectories of the spectrum in the energy plane as illustrated in Figure 2 provide the major clue for an understanding. Within the range of interest for real  $\lambda$ -values the two peaks pointing in opposite directions are well described by

$$E_{\pm}(\lambda) \approx E_r \pm \sqrt{(\lambda - \lambda_-)(\lambda - \lambda_+)}, \quad (3)$$

where

$$\lambda_{\pm} = \mp \frac{i(\omega_1 - \omega_2)}{2\delta \pm i(\epsilon_1 - \epsilon_2)}$$

are the two EPs. For small  $\delta$  they lie near to each other and degenerate into a single diabolic point when the coupling parameter  $\delta$  vanishes. The constant  $E_r$  ensures that both energies have a negative imaginary part for real  $\lambda$  to allow their interpretation as true resonances. Notice that care has to be taken for the values to remain in the same Riemann sheet in a numerical generation of a plot like the one in Figure 2 where real values of  $\lambda$  are used. At the critical point  $\lambda_{cr}$  – that is where the two tips of the two peaks occur – one energy value is very close to the real axis while the other is more remote from the real energy axis. These two pole terms occur in the Green’s function, and it is here where the corresponding residues play a decisive role. The analytical expressions for the residues blow at the EPs like  $1/\sqrt{(\lambda - \lambda_+)(\lambda - \lambda_-)}$  owing to the vanishing norms of the eigenstates. We give a simplified expression representing numerically the correct analytical terms quite well for real  $\lambda$ . It reads

$$r_{\pm}(\lambda) \approx \frac{1}{2} \pm \frac{A}{\sqrt{\lambda - (\lambda_+ + \lambda_-)/2}} \quad (4)$$

where the constant  $A$  is suitably adjusted yielding  $|r_+(\lambda)| \lesssim 1$  at  $\lambda_{cr}$ . A combined diagram of the real functions  $|r_+(\lambda)|$  and  $|r_-(\lambda)|$ , as a function of  $\Re\lambda$ , looks similar in shape to Figure 2 with the difference that the peaks reach near unity and zero, respectively. The diagonal elements of the full Green’s function are then given by

$$\begin{aligned} (E - H)_{11}^{-1} &= \frac{r_+(\lambda)}{E - E_+(\lambda)} + \frac{r_-(\lambda)}{E - E_-(\lambda)} \\ (E - H)_{22}^{-1} &= \frac{r_-(\lambda)}{E - E_+(\lambda)} + \frac{r_+(\lambda)}{E - E_-(\lambda)} \end{aligned} \quad (5)$$

while the corresponding poles of the off-diagonal terms have the residues  $\sqrt{r_+(\lambda)r_-(\lambda)}$ . With the insight from equations (3)–(5) we qualitatively understand the shapes of Figure 3. The strong peak (left) originates from the near pole at  $E_+(\lambda_{cr})$  with its strong residue  $r_+(\lambda)$ . The right hand figure is produced by the remote pole at  $E_-(\lambda_r)$  with its strong residue while the small peak on top is generated by the near pole with the very small residue. The rather dramatic  $\lambda$ -dependence is due to the proximity of the EPs; of course this is related to the actual value of the coupling  $\delta$  and will have a sensitive dependence on  $\delta$  at  $\lambda = \lambda_{cr}$ . Note that, if the coupling in our two-dimensional model is further increased, the narrow resonance is eventually crossing the real energy axis and acquires a positive imaginary part. It then can no longer be interpreted as a decaying state, that is as a physical resonance. It may be interpreted, for example, as an inversely populated level producing light amplification generated by a radiation process in laser physics [22].

### 3 Conclusion

Let us discuss a few cases where the phenomena described in this paper have been encountered. In a model for quantum transport [23], transmission increases drastically for

a specific width of some external barriers simulating the coupling strength of the system with the environment; this parameter plays the role of our  $\lambda$ . The authors stress that the complex eigenvalues of the effective Hamiltonian are very important for understanding the transport properties of the system. The analysis is based in part on findings of [24] where the sensitive dependence upon the threshold energy of the continuum coupling for loosely bound nuclei has been demonstrated using an effective two by two non-Hermitian Hamiltonian. In [3] a specific frequency of the laser beam leads to the occurrence of a ‘resonance’ pole with zero width; within its immediate vicinity this parameter can be rewritten as our parameter  $\lambda$ . The quoted paper concentrates on specific solutions of the Schrödinger equation, which are in fact the Gamow states (only outgoing waves as boundary conditions). They correspond to the poles of the Green’s function in our two-level model (which has of course no continuous spectrum). In all these cases, the extremely strong dependence on the coupling of the pole positions close to or upon the real axis, is the effect of near exceptional points. The openness of the systems is crucial for all these phenomena.

In summary, the dramatic features of particular resonance behaviour are explained by the square root singularities of spectrum and eigenstates, especially the vanishing norm of the latter that gives rise to the dramatic and distinctly different behaviour in each channel. In a two channel problem, that was chosen as a typical case, they invoke strong dependence on the interaction strength and significant deviations from the usual patterns associated with isolated or overlapping resonances.

WDH is thankful for the hospitality which he received from the Nuclear Theory Section of the Bogoliubov Laboratory, JINR during his visit to Dubna. This work is partly supported by JINR-SA Agreement on scientific collaboration, by Grant No. FIS2008-00781/FIS (Spain) and RFBR Grants No. 08-02-00118 (Russia).

## References

1. R.G. Newton, *Scattering Theory of Waves and Particles* (Springer-Verlag, New York, 1982)
2. C. Mahaux, H. Weidenmüller, *Shell-Model Approach to Nuclear Reactions* (North-Holland, Amsterdam, 1969)
3. A. Mostafazadeh, Phys. Rev. Lett. **102**, 220402 (2009)
4. W.D. Heiss, Eur. Phys. J. D **7**, 1 (1999)
5. W.D. Heiss, Phys. Rev. E **61**, 929 (2000)
6. W.D. Heiss, Czech. J. Phys. **54**, 1091 (2004).
7. A.A. Mailybaev, O.N. Kirillov, A.P. Seyranian, Phys. Rev. A **72**, 014104 (2005)
8. U. Günther, I. Rotter, B.F. Samsonov, J. Phys. A: Math. Theor. **40**, 8815 (2007)
9. E.A. Solov’ev, Sov. Phys. Usp. **32**, 228 (1989)
10. H. Cartarius, J. Main, G. Wunner, Phys. Rev. A **79**, 053408 (2009)
11. M.V. Berry, D.H.J. O’Dell, J. Phys. A **31**, 2093 (1998)
12. J. Okolowicz, M. Płoczejczak, Phys. Rev. C **80**, 034619 (2009)
13. M. Znojil, Phys. Lett. B **647**, 225 (2007)
14. W.D. Heiss, F.G. Scholtz, H.B. Geyer, J. Phys. A: Math. Gen. **38**, 1843 (2005)
15. P. Cejnar, S. Heinze, M. Macek, Phys. Rev. Lett. **99**, 100601 (2007)
16. C. Dembowski, H.-D. Gräf, H.L. Harney, A. Heine, W.D. Heiss, H. Rehfeld, A. Richter, Phys. Rev. Lett. **86**, 787 (2001)
17. C. Dembowski, B. Dietz, H.-D. Gräf, H.L. Harney, A. Heine, W.D. Heiss, A. Richter, Phys. Rev. E **69**, 056216 (2004)
18. S.-B. Lee, J. Yang, S. Moon, S.-Y. Lee, J.-B. Shim, S.W. Kim, J.-H. Lee, K. An, Phys. Rev. Lett. **103**, 134101 (2009)
19. E. Hernandez, A. Jaureguit, A. Mondragon, J. Phys. A **33**, 4507 (2000)
20. W.D. Heiss, J. Phys. A: Math. Gen. **37**, 2455 (2004)
21. T.V. Shahbazyan, M.E. Raikh, Phys. Rev. B **49**, 17123 (1994)
22. H. Cao, J. Phys. A: Math. Gen. **38**, 10497 (2005)
23. G.L. Celardo, L. Kaplan, Phys. Rev. B **79**, 155108 (2009)
24. A. Volya, V. Zelevinsky, Phys. Rev. C **67**, 054322 (2003)